Plant Physiology and Biochemistry 130 (2018) 623–632

Contents lists available at ScienceDirect

Plant Physiology and Biochemistry

journal homepage: www.elsevier.com/locate/plaphy

Research article

Starch accumulation is associated with active growth in *A. tequilana*

Laura E. Zavala-García, Lino Sánchez-Segura, Emmanuel Avila de Dios, Arely Pérez-López, June Simpson*

Department of Genetic Engineering, Cinvestav Unidad Irapuato, Km. 9.6 Libramiento Norte Carretera Irapuato-León, Apdo. Postal 629, 36821, Irapuato, Guanajuato, Mexico

ARTICLE INFO

Keywords:
Starch metabolism
A. tequilana
Primary thickening meristem
SAM
In silico expression
Histological analysis

ABSTRACT

Transcriptome analysis of different tissues and developmental stages of *A. tequilana* plants led to the identification of full length cDNAs and the corresponding amino acid sequences for enzymes involved in starch metabolism in this species. Comparison with sequences from other species confirmed the identities of putative *A. tequilana* starch metabolism genes and uncovered differences in the evolutionary patterns of these genes between gramineous and non-gramineous monocotyledons. *In silico* expression patterns showed high levels of expression of starch metabolism genes in shoot apical meristem tissue and histological studies showed the presence of starch in leaf primordia surrounding the shoot apical meristem and in the primary thickening meristem of the stem. Starch was also found to accumulate significantly in developing floral organs and immature embryos. Low levels of starch were observed overall in leaf tissue with the exception of stomatal guard cells where starch was abundant. In root tissue, starch was only observed in statoliths at the root tip. *A. tequilana* starch grains were found to be small in comparison to other species and have an almost spherical form. The data for gene expression and histological localization are consistent with a role for starch as a transient carbohydrate store for actively growing tissues in *A. tequilana*.

1. Introduction

Agave species have been exploited in Mexico since the pre-hispanic era (Gentry, 1982; García-Mendoza, 1992, 2000; García, 2011) and are currently of commercial importance for the preparation of alcoholic beverages such as tequila and mescal (https://www.crt.org.mx/, http://www.crm.org.mx/). Most *Agave* species are perennial and monocarpic with life cycles ranging between 5 and 50 years and are well adapted to dry marginal terrain having shallow roots, leaves organized in rosette formation, thick cuticles and crassulacean acid metabolism (CAM) (Gentry, 1982). *Agaves* are also included in the 15% (Hendry, 1987, 1993; Brocklebank and Hendry, 1989) of angiosperms that store carbohydrates in the form of fructans which are predominantly stored in the expanded stem structure but are also found in almost all organs including leaves, roots and floral tissue (Avila de Dios et al., 2015; Mancilla-Margalli and Lopez, 2006). Low molecular weight fructans can be mobilized from leaves through the phloem (Wang and Nobel, 1998) and in addition to carbohydrate storage fructan polymers are thought to have roles in stress tolerance, regulation of osmosis and signaling (Van den Ende and Valluru, 2009; Van den Ende et al., 2004; Van den Ende, 2013; Van den Ende, 2014).

In contrast to *Agave* species, the majority of angiosperms store carbohydrates both transiently and long-term in the form of starch (Zeeman et al., 2010). Transient starch storage occurs in leaves and stems where levels can be modulated in accordance with the needs of the plant, whereas long-term storage is associated with specific organs such as seeds, roots or tubers (Zeeman et al., 2010). Within the monocotyledons starch metabolism has evolved differently within distinct taxonomic groups (Comparot-Moss and Denyer, 2009). The Commelinid clade which houses gramineous species such as cereals, sedges and banana species is characterized by species that produce seeds with starch-rich endosperm tissue. Other monocotyledonous clades however, including the Asparagales (containing the *Agave* genus) and Lilliales do not significantly accumulate starch in seed endosperm. ADPglucose is an essential starch precursor synthesized in the chloroplasts of all angiosperms. Gramineous species however, are further distinguished by the ability to also synthesize this molecule in the cytosol due to the presence of an extra AGPase enzyme in this compartment, indicating fundamental differences in the evolution of starch metabolism encoding genes in gramineous and non-gramineous

* Corresponding author.
E-mail addresses: elizavala1993@gmail.com (L.E. Zavala-García), lino.sanchez@cinvestav.mx (L. Sánchez-Segura), aviladedios@gmail.com (E. Avila de Dios), arely.perez@cinvestav.mx (A. Pérez-López), june.simpson@cinvestav.mx (J. Simpson).

https://doi.org/10.1016/j.plaphy.2018.08.011
Received 13 March 2018; Received in revised form 7 August 2018; Accepted 7 August 2018
Available online 11 August 2018

monocotyledons (Comparot-Moss and Denyer, 2009; James et al., 2003).

Several monocotyledonous species synthesize both starch and fructans and starch localization and metabolism has been studied in some fructan producing monocotyledons including grass species such as wheat (*T. aestivum*) (Scofield et al., 2009) and non-gramineous species such as onion (*A. cepa*) and Asparagus (Schnabl and Ziegler, 1977; Zhang et al., 2016) (Ernst et al., 1998, 2003; Ernst and Krug, 1998) where some evidence for both spatial and temporal separation of starch and fructan metabolism has been uncovered.

Agave species in common with *Allium* species are non-gramineous monocotyledons found in the Asparagales clade. Although these species do not accumulate starch in endosperm tissue or other specialized organs, it could be expected that starch would be transiently synthesized in leaves as a consequence of photosynthesis in these species. However Christopher and Holtum (1996) reported that starch is not stored in *Agave guadalajarana* leaves and only low levels of starch are detected in *A. tequilana* stems (Mancilla-Margalli and López, 2006). Additionally in *A. cepa* (a species relatively closely related to the *Agave* genus), the absence of starch in stomatal guard cells has been reported (Schnabl and Ziegler, 1977; Schnabl et al., 1978; Schnabl, 1980).

The localization and role of starch metabolism in *Agave* species is therefore unclear and since there is a growing interest in the use of Agaves as renewable bioenergy sources (Yang et al., 2015; Liu et al., 2015; Cushman et al., 2015; Davis et al., 2011) based on their capacity for biomass production (a trait linked directly to photosynthesis and carbohydrate metabolism) and the possibility to exploit marginal land, a fundamental knowledge of the roles of both fructan and starch metabolism in these species and how they interact is essential. This report begins to address this problem by characterizing cDNA sequences and determining *in silico* expression patterns in *A. tequilana* for genes encoding key enzymes in starch metabolism and describing the pattern of starch localization and the size and shape of the starch grains observed based on the histological analysis of different organs and tissues of this species. The results confirm a distinct pattern of evolution for starch metabolism genes between gramineous and non-gramineous monocotyledonous species and patterns of starch localization in combination with *in silico* expression data lead us to suggest that starch rather than fructans is the primary carbohydrate source exploited in actively growing tissues of *Agave* species.

2. Materials and methods

2.1. Plant material

For vegetative tissues, samples for histochemical and microscopical analysis were obtained from at least three, two-year old greenhouse grown *A. tequilana* plants (Supplementary Fig. 1a). For each plant, samples were obtained from: the leaf base and middle section of 2 individual leaves (both adaxial and abaxial areas), the center of the stem, the center and tip of the root, the shoot apical meristem (SAM) and rhizome tissue. Additionally adaxial and abaxial epidermis from middle-leaf tissue (Supplementary Fig. 1b), were analyzed. Depending on the tissue both transversal and longitudinal sections were obtained and were either fixed or analyzed as fresh tissue. Samples for analysis of floral structures (umbel, inflorescence, immature bud, seeds) were obtained from mature plants with an inflorescence showing floral buds (Supplementary Figs. 1c and d).

2.2. Multiphoton microscopy and rhodamine B staining

Samples were imaged on a multiphoton microscopy system (LSM 880NLO, Zeiss, Germany) equipped with a Ti: Sapphire laser (Chameleon vision II, COHERENT, Scotland) capable of tuning in ranges from 690 to 1060 nm. *A. tequilana* tissues were observed with a short working distance objective 20X/0.5, NA ∞-0.17, Zeiss Plan NEOFLUAR and starch localization was carried out with an immersion objective 40X/1.3, NA ∞-0.17, Zeiss Plan NEOFLUAR. The rhodamine B spectrum was obtained from the data-base of Zeiss microscope dyes. The spectrum was divided into two ranges, small window detection from 547 to 602 nm for visualization of cells walls and cuticle (in green) and large window detection from 600 to 735 nm for visualization of starch grains (in magenta) (Supplementary Fig. 2). All micrographs were captured in .CZI format at 1131x1131 pixels and RGB colour.

For the emission spectrum analysis of starch, 1 mg of potato starch grains (Merck, Germany) was mixed with 100 μL of ethanol/rhodamine solution (Hycel, Mexico) at 0.01% and incubated for 5 min, at room temperature. Subsequently the sample was washed three times with deionized water. The *A. tequilana* tissues (leaf primordia, expanded leaf and root) were dissected in 2 mm thick sections and dehydrated in a series of ethanol solutions (from 10 to 50%) for 30 min at room temperature. Subsequently, samples were incubated in an ethanol–glycerine-water solution, in ratios of 1:1:2, 1:1:1 for 12 h, in the final step absolute ethanol and glycerine were added in equal proportions (1:1) and samples were incubated for 24 h. Tissues were washed three times with a 50% ethanol solution and incubated in 1 mL of ethanol-acetone rhodamine solution at 0.01% for 10 min at room temperature. The staining process was completed by washing samples and leaving them for 72 h in deionized water at 4 °C. The tissues were mounted on glass slides, covered with high performance Zeiss cover glasses (D = 0.17 mm ± 0.005 mm refractive index = 1.5255 ± 0.0015, Abbe number = 56 ± 2) and observed in a multiphoton microscope.

2.3. Lugol staining

Apical, middle and basal *Agave tequilana* leaf tissue was dissected and incubated in graded solutions of sucrose (10–30%) dissolved in phosphate buffer at 0.16 M, pH 7.4 for 2 h at 4 °C. Subsequently, samples were embedded in LEICA tissue freezing medium (Leica Biosystems, United Kingdom) and frozen at −35 °C for 10 min. Tissues were cut in sections of 30 μm with high profile microtome 818 blades (Leica Microsystems, Germany). For starch detection, samples were incubated with lugol solution (1% in 50% ethanol) for 15 min and washed for 30 min.

Freehand sections of around 5 mm were obtained for umbel, floral meristem, root, stem and leaf tissues. Samples were incubated with lugol solution (1% in 50% ethanol) for 15 min, washed for 30 min and mounted on glass slides. Samples were observed in a Keyence VHX5000 digital microscope (Keyence, Japan), at 200X amplification (VH-Z20R, Keyence, Japan) with LED illumination.

2.4. Paraffin sections

The protocol was modified from (Sánchez-Segura et al., 2015). Root, central stem, basal and middle leaf tissues of *A. tequilana,* as well as positive controls rice (grain) and potato (tuber) were fixed during 24 h in 4% paraformaldehyde (Electron Microscopy Sciences, USA) dissolved in phosphate buffer, pH7.2 for 12 h, after which they were washed three times with phosphate buffer during 30 min at room temperature. Subsequently, the samples were dehydrated in a graded ethanol series (from 10% to 100%) and cleared with xylol and infiltrated with xylol-paraplast (2:1, 1:1, 1:2 and pure paraplast). Residual xylol was evaporated during 24 h at 60 °C, before embedding in pure Paraplast (McCormick Scientific, USA). Blocks were cut to 10 μm in width in a rotary retracting microtome (Liljeholmen, Kema and Bryggerierna (LKB), Sweden). The paraffin ribbons were de-waxed and cleaned in xylol, the rehydration of the sections was carried out in ethanol solutions (from 100% to 50%) and samples were stained with Lugol solution as described above and mounted in Entellan resin (Merck, Germany). The sections were examined under a light microscope (Olympus, BX50-BF, Japan) with an Infinity3 camera 1.4 MP (Lumenera, Canada) and ImagePro Premier 9.1 (Media Cybernetics,

USA) program.

2.5. PAS staining

Samples for Periodic Acid-Schiff (PAS) staining of fresh tissue were obtained by freehand sectioning and carried out using a kit obtained from Sigma Cat. Núm 395B SIGMA® containing a solution of hematoxilin Gill No.3, periodic acid and Schiffs reagent. Tissue sections of 20–50 μm were obtained and incubated in periodic acid solution (0.5% v/v) for 8 min., rinsed twice in distilled water for 5 min. then submerged in Schiffs reagent 50% v/v for 5 min. Samples were then rinsed in distilled water and mounted on slides for observation on an BX60 microscope Olympus (Olympus, Japan) F5, equipped with digital camera (Olympus U-CMAD-2, Japan) and analyzed using Image-Pro plus versión 6.2.

2.6. Morphometric analysis of starch grains

All images of starch grains in sections of *A. tequilana*, rice and potato tissues stained with lugol were cropped by using Corel Paint Shop Pro Photo XI (V11.0, Corel Corporation, USA) software and transferred into a new image with a white background. Morphometric analysis of 300 starch grains was carried out for each plant species with Sigma Scan Pro (V5.0, SPSS, USA) software and calibrated with a micrometre reference (Nikon, Japan) to obtain the relation pixels-μm. The descriptors measured were area and shape factor. Average ± standard deviation values of each parameter were reported and analyzed statistically applying Kolmogorov-Smirnov, Kruskal-Wallis and Mann-Whitney tests using Sigma Stat. Data obtained for 30 images were entered in an Excel worksheet.

2.7. Bioinformatic analysis

Sequences encoding enzymes involved in starch metabolism were obtained from Illumina-generated RNA-seq data from different *A. tequilana* tissues and developmental stages (Avila de Dios et al. unpublished). Reads were mapped to the transcriptome using the script "alignreads.pl" from the suite of scripts of the Trinity assembly tool, the program which uses the script to map the reads was Bowtie 2 and alignments were only considered valid when both reads aligned to the same transcript. The TPM values were calculated using RSEM, which is integrated into the alignreads.pl script. Sequences were manually aligned to recover full-length transcripts and corresponding amino acid sequences using Geneious Version R8 http://www.geneious.com (Kearse et al., 2012). Dendrograms were produced from pairwise alignments of full-length amino acid sequences using MUSCLE and UPGMA with bootstrap analysis involving 1000 repetitions. Full-length nucleotide and amino acid sequences for *A. tequilana* starch metabolism genes have been deposited in GenBank under the accession numbers shown in Table 1. *In silico* expression analysis was determined directly from the RNA-seq data in transcripts per million and one-way ANOVA was applied to determine significant differences in expression levels between different tissues.

3. Results

3.1. Determination of tissues associated with starch metabolism in A. tequilana based on gene expression data

In order to optimize the choice of tissues to be sampled for histological analysis, cDNA sequences encoding key enzymes involved in starch metabolism were identified from RNA-seq data, confirmed by comparison of full-length amino acid sequences with those from other species and used to determine *in silico* expression patterns.

Table 1 summarizes the enzymes for which full-length amino acid sequences based on *A. tequilana* transcriptome data could be determined. These sequences were used for comparison with sequences available in public databases encoding the same enzyme types to produce the dendrograms presented in Supplementary Fig. 3 a–h.

Table 1
Summary of isoforms identified for starch metabolism genes in *A. tequilana* transcriptome databases.

Enzyme Type	*A. tequilana* gene	GenBank Accession number
Adenosine Diphosphate Glucose Pyrophosphorylase 1 small subunit	*AtqAGPS1*	MH647770
Adenosine Diphosphate Glucose Pyrophosphorylase 1 large subunit	*AtqAGPL1*	MH635253
Adenosine Diphosphate Glucose Pyrophosphorylase 3 large subunit	*AtqAGPL 3*	MH635254
Granule Bound Starch Synthase I	*AtqGBSSI*	MH635255
Soluble Starch Synthase 1	*AtqSSS1*	MH635256
Soluble Starch Synthase 2	*AtqSSS2*	MH647771
Soluble Starch Synthase 4	*AtqSSS4*	MH647772
Starch Branching Enzyme II	*AtqSBEII*	MH635257
Isoamylase-3	*AtqISA3*	MH647774
Alpha-amylase 3	*AtqAAM3*	MH635258
Beta-amylase 3	*AtqBAM3*	MH647775
Beta-amylase 8	*AtqBAM8*	MH647773

Three isoforms were identified for Soluble Starch Synthase (SSS), Two isoforms encoding Adenosine Diphosphate Glucose Pyrophosphorylase large subunit (AGPL) and two isoforms for B-amylase (BAM, AtqBAM3-predicted chloroplast localization and AtqBAM8-predicted cytosol localization) and single isoforms were identified for Adenosine Diphosphate Glucose Pyrophosphorylase small subunit (AGPS), A-Amylase (AAM, AtqAAM3-predicted chloroplast isoform), Isoamylase (ISA) and Starch Branching enzyme (SBE) (Supplementary Fig. 3 a–h). For all enzymes and all isoforms, the *A. tequilana* proteins are most closely related to proteins from other non-gramineous monocotyledons, however interestingly in several cases (indicated by dashed boxes in Supplementary Fig. 3), the non-gramineous monocotyledon group is more closely related to dicotyledonous species (indicated by non-solid boxes in Supplementary Fig. 3) than to the gramineous monocotyledons and for some specific isoforms of different enzyme types, the gramineous monocotyledons form discrete, separate clades (indicated by solid boxes in Supplementary Fig. 3). The dendrograms presented confirm the identity of the enzymes summarized in Table 1, therefore ensuring that the *in silico* expression analysis based on these sequences is robust.

3.2. In silico expression analysis of genes encoding enzymes involved in starch metabolism in A. tequilana

Based on the assumption that the pattern of expression of the genes involved in starch metabolism reflects the presence of starch in different tissues, *in silico* expression analysis based on RNA-seq data was carried out for each enzyme isoform identified. Fig. 1 where data are normalized in relation to each individual tissue type shows that in Shoot Apical Meristem (SAM) tissue the greatest number of genes involved in starch metabolism show their highest levels of expression, followed by leaves and roots. This unexpected result led us to analyze in greater detail the expression patterns of starch metabolism enzymes in SAM tissue during developmental changes between the vegetative and reproductive stages of *A. tequilana*. RNA-seq data is available for leaf and SAM tissue at 3 different stages of the vegetative to reproductive transition: VL and VM-vegetative leaf and meristem respectively, SL and SM, leaf and meristem tissue from "Sunken" or initial stage of bolting and IL and IM, leaf and meristem tissue from plants with an inflorescence of 10 cm. In this case data are shown for enzyme type rather than specific isoforms. The results shown in Supplementary Fig. 4 are consistent with those shown in Fig. 1 where significant differences (indicated by *) were found between leaf and SAM tissue for 4

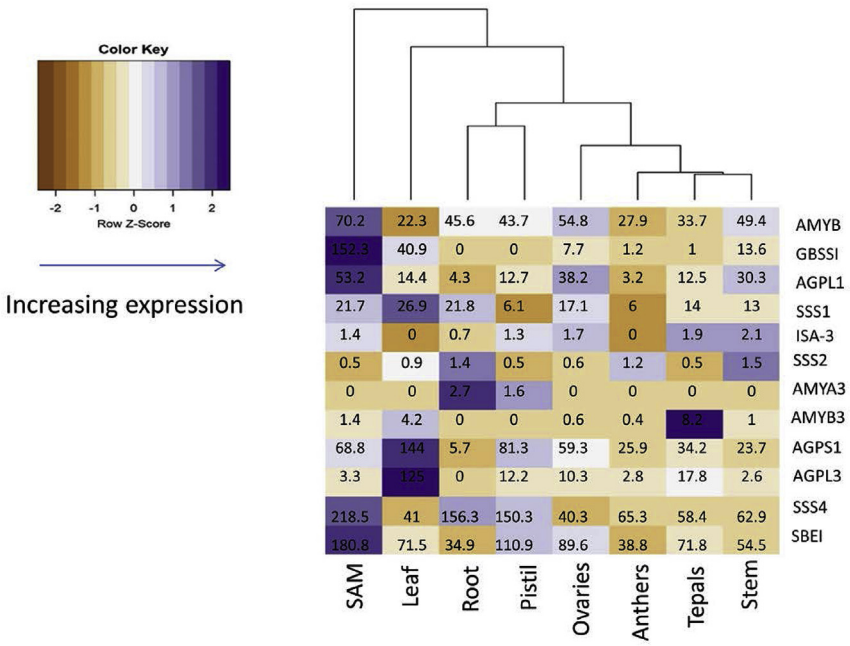

Fig. 1. *In silico* analysis of expression of starch metabolism genes. Heat diagram depicting levels of expression of each gene associated with starch metabolism in relation to different plant organs. Darker purple indicates highest levels of expression and numbers show the TPM/RPM for each gene/tissue combination. AGPL- Adenosine Diphosphate Glucose Pyrophosphorylase large subunit, AGPS-Adenosine Diphosphate Glucose Pyrophosphorylase small subunit, BAM-B-amylase, AAM-A-amylase, GBSS-Granule bound starch synthase,. SSS-Soluble starch synthase, SBE-Starch branching enzyme, ISA-Isoamylase. (For interpretation of the references to color in this figure legend, the reader is referred to the Web version of this article.)

different types of enzyme (AGPL, GBSS, ISA and B-AMY). AGPS was significantly expressed at a higher level in the SAM at the initial stage of development of the inflorescence (SM) in comparison to all other stages in both leaves and SAM. SSS genes showed significantly reduced expression in leaf tissue at the 10 cm inflorescence stage (IL) in relation to all other stages in both leaves and SAM. These data confirm the high levels of expression observed for specific starch metabolism genes in SAM tissue and indicate that during the developmental transition between the vegetative stage and the reproductive stage, levels of expression of starch metabolism genes in leaf tissue remain constant with the exception of the noted reduction in expression of SSS when the inflorescence is already established.

3.3. Localization of starch in A. tequilana

Based on the expression patterns of starch metabolism genes, histological examination of the presence of starch could be directed towards specific organs and tissues and Lugol's iodine solution and rhodamine fluorescence were used as described in Materials and Methods to carry out this analysis.

The strong expression of starch metabolism genes in the SAM suggested that starch would be present in this tissue. In order to accurately locate starch, whole stem tissue of 2 year old *A. tequilana* plants were treated with Lugol's solution. As shown in Fig. 2a, a, b, c and d, starch is located in the leaf primordia surrounding the SAM and is specifically associated with vascular tissue (Fig. 2a, e, f, g and h), (Supplementary Fig. 6, a-h). A ring of starch containing cells is also observed around the periphery of the stem in the region below the leaves that corresponds to the primary thickening meristem (PTM) (Fig. 2a, i and j) indicated with* in Fig. 2a, j. The PTM forms a layer surrounding underlying stem tissue and starch is also observed in association with vascular tissue extending from the PTM Fig. 2a, f and h). At higher magnification discrete starch grains can be observed in the PTM (Fig. 2a, k and l).

The starch layer also forms initially around the meristem of new rhizomes as shown in Fig. 2a, j and indicated as (+). Mature rhizome tissue however (Supplementary Figs. 5b–f) shows some staining close to vascular tissue, but does not show a well-defined PTM when stained with lugol. In contrast PAS staining for total carbohydrates including both starch and fructans strongly stains the whole stem and rhizome (Supplementary Fig. 5 e an f).

Root tissue showed Lugol staining only at the extreme root tip but not in other root cells (Fig. 2b, a-d and Supplementary Fig. 6, q-t), closer inspection revealed that this corresponds to the presence of starch in statoliths (Fig. 2b, d) and not the root meristem *per se*.

In order to determine the presence of starch in photosynthetic and non-photosynthetic sections of *A. tequilana* leaves, both adaxial and abaxial surfaces of middle and basal leaf sections were examined as shown in Supplementary Fig. 1a. As can be observed in Fig. 3a and b and Supplementary Fig. 6, i-p starch is more abundant in cells directly below the epidermal layer in both green and white leaf tissue. This was consistent for both abaxial and adaxial surfaces. Images of epidermal tissue taken from both adaxial and abaxial surfaces of green leaf tissue clearly show Lugol staining of the guard cells (Fig. 3c and d and a detailed image by multiphoton microscopy of the stomatal structure of guard cells in an *A. tequilana* leaf clearly shows the sunken guard cell anatomy typical of many CAM plants and the presence of starch in the guard cells but not in subsidiary cells in green leaf tissue (Supplementary Fig. 6, i-l). Starch grains were also observed in some but not all of the chloroplasts in samples from cells in internal layers of green leaf tissue (Fig. 3e and f) and in a few cells surrounding some vascular tissue (Supplementary Fig. 6, e-h). In basal, white (non-photosynthetic) leaf tissue starch was also observed in stomatal guard cells (Supplementary Fig. 6, m-p) but granules of starch could not be observed in cells in internal layers by staining with lugol in comparison to green tissue (Fig. 3g and h). The low level of accumulation of starch in green leaf tissue and absence of accumulated starch in white leaf tissue suggests the in *A. tequilana* leaves starch is used for transient storage of carbohydrates before being broken down for consumption or transport to sink organs. Negative controls are shown in Supplementary Fig. 5.

Gene expression results also indicated active starch metabolism in floral tissue and lugol staining of inflorescence, umbels and flower buds revealed strong staining of flower buds (Fig. 4 a and b) and the presence of starch in peripheral meristem and vascular tissue of umbels (Fig. 4 c and d). *A. tequilana* produces white (normally non-viable) seeds and black (viable seeds), only black seeds contain endosperm and embryo tissue. Interestingly the SAM region of the developing embryo was clearly stained in immature seeds but not in mature seeds (Fig. 4 e–h) whereas endosperm tissue from either immature or mature seeds did not stain strongly with lugol. However, endosperm and embryo tissue of mature seeds stain strongly with PAS (Supplementary Fig. 7), indicating the presence of carbohydrates other than starch in this tissue.

The inflorescence stalk did not show significant staining with lugol

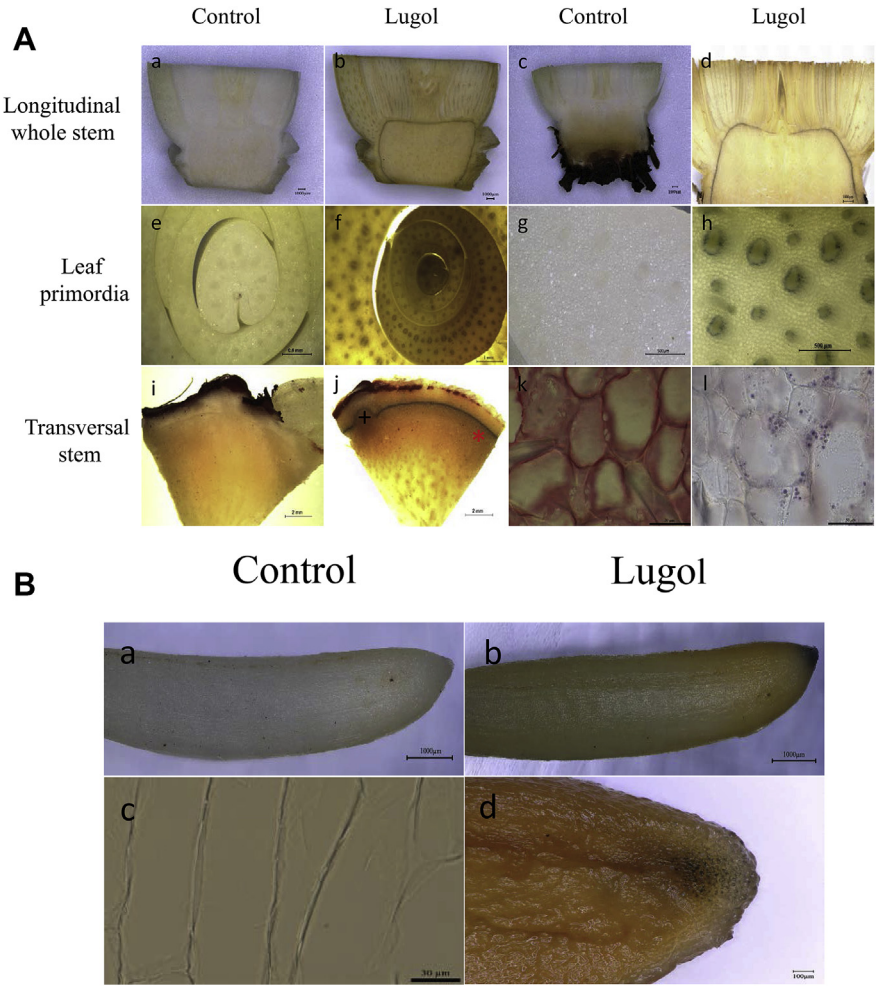

Fig. 2. a. Lugol staining of SAM and stem tissue. a,b. Longitudinal whole stem section, c,d. Longitudinal higher magnification image of SAM, e,f. Transverse section of leaf primordia at SAM, g,h. Higher magnification image of transverse section of leaf primordia at SAM, i,j. Transversal image of stem section, k,l. Higher magnification of PTM region. * indicates PTM, + indicates new root meristem. a,c,e,g,i,k-controls without Lugol staining, b,d,f,h,j,l-Lugol stained tissue. **b. Lugol staining of root tissue.** a and b-whole root tip, c-internal root cells, d-root tip showing statoliths.

(Fig. 4e and f).

A wide range of forms and sizes of starch grains have been reported in different plant species and in order to determine where within this spectrum the starch grains from *A. tequilana* lie, measurement of the size and shape of starch grains were carried out as described in Materials and Methods and compared to 2 control species (potato, *Solanum tuberosum* and rice, *Oryza sativa*).

Fig. 5 a and b shows the comparison of the average sizes of starch grains recorded for *A. tequilana* in comparison to those of potato and rice. As can be observed the *A. tequilana* starch grains are slightly smaller (3X) than those of rice and significantly (53X) smaller than those of potato. In terms of shape Fig. 5c shows that on average *A. tequilana* starch grains approximate more closely to a spherical shape (average s value 0.902) than starch grains measured either in rice (average s value 0.783) or potato (average s value 0.832), an s value of 1 represents a perfect sphere.

4. Discussion

Previous reports have shown that starch accumulation in leaf and stem tissue of some *Agave* species is negligible (Christopher and Holtum, 1996; Mancilla-Margalli and López, 2006) and initial attempts in our laboratory to directly detect starch in different organs, including leaves, stems and roots of *A. tequilana* proved to be only marginally successful in leaf tissue. Characterization of cDNAs and expression patterns of genes encoding enzymes involved in starch metabolism proved to be a successful strategy not only to identify tissues where starch is localized but also to shed light on some aspects of the evolution of genes involved in starch metabolism. Earlier reports (Li et al., 2012) have largely compared only starch metabolism gene sequences obtained from gramineous monocotyledons and dicotyledonous species whereas the present report includes several examples of non-gramineous monocotyledons for genes of each enzyme type. As expected the *Agave tequilana* sequences are most closely related to other non-gramineous monocotyledonous species such as onion, asparagus or banana. Interestingly, for some isoforms the non-gramineous groups are more closely related to dicotyledonous species rather than the gramineous monocotyledons. Specific groups containing only isoforms from gramineous monocotyledons genes were also identified. These results agree well with the evolutionary pattern proposed for monocotyledons where gene duplications specifically within the gramineous monocotyledon group have led to a diversification in genes and enzymes including those involved in starch metabolism (Comparot-Moss and Denyer, 2009)allowing high levels of starch to be produced in seed endosperm (Li et al., 2003). The results suggest that within the monocotyledons evolutionary patterns for at least some isoforms of genes encoding enzymes involved in starch metabolism are quite distinct.

Surprisingly RNA-seq data revealed the high levels of several starch metabolism genes in SAM tissue. The SAM tissue used for RNA-seq analysis also included leaf primordia at the very earliest stages since it

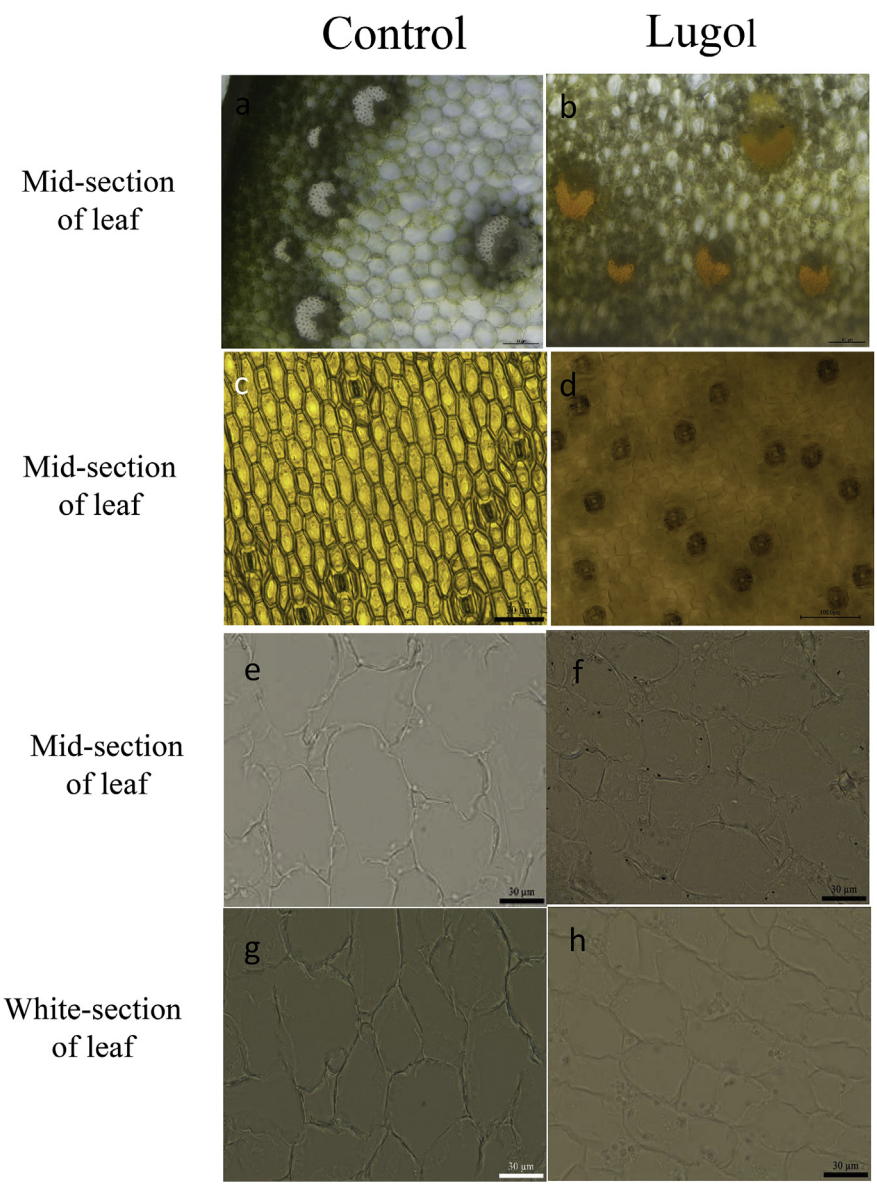

Fig. 3. Localization of starch in leaf tissue using Lugols reagent. a,c,e,g lugol stained tissues, b,d,f,h un stained controls. a,b. epidermis, c,d. transverse section of *A. tequilana* leaf, e,f internal section of green *A. tequilana* leaf, g,h. internal section of basal (white) *A. tequilana* leaf. (For interpretation of the references to color in this figure legend, the reader is referred to the Web version of this article.)

is difficult to isolate only the SAM. Detailed histological analysis showed that starch is located in the PTM, a region associated with leaf and root growth and expansion of the stem tissue (Cattai and Menezes, 2010; de Menezes et al., 2005). The PTM and SAM come together at the SAM, however cells localized within the SAM itself do not show the presence of starch. Analysis of whole stem tissue revealed a layer of starch located at or close to the PTM, which encloses the underlying stem tissue and in association with vascular tissue that connects to the PTM. These observations suggest that a reservoir of starch is maintained in PTM tissue to be exploited as an energy source as needed for actively growing tissues. The specific localization of starch in the PTM is also consistent with the report of Mancilla-Margalli et al. (Mancilla-Margalli and López, 2006) where very low levels of starch were reported in the center of the stem which does not include the PTM.

Rhizome tissue does not show significant accumulation of starch in the region corresponding to the PTM although some starch is present close to vascular tissues. This result contrasts with observations in stem tissue and may indicate that starch accumulates in rhizome tissue only as a transient reserve that is then mobilized towards the growing rhizome tip or for the initiation and development of offsets.

The accumulation of other carbohydrates (probably fructans) in rhizome tissue may provide a log term reserve for growth and development of offsets but may also be involved in providing drought tolerance. In roots, starch is only observed at the root tip in the gravity sensing statoliths but is not associated with the root apical meristem (RAM).

Expression analysis also revealed the presence of starch metabolism related transcripts in floral tissues and the presence of starch was also confirmed by lugol staining in umbels and developing flower buds, consistent with an association with actively growing tissues. Observation of both developing and black seeds, which are normally viable in comparison to white seeds (Escobar-Guzmán et al., 2008) showed specific lugol staining of the SAM region of the embryo of immature seeds but not mature seeds suggesting that in the developing embryo starch is also transiently stored during embryo growth but is absent from both the embryo and endosperm tissue in mature, dormant seeds. PAS staining indicates the presence of carbohydrates in endosperm and embryo tissue of mature seeds that must supply the needs

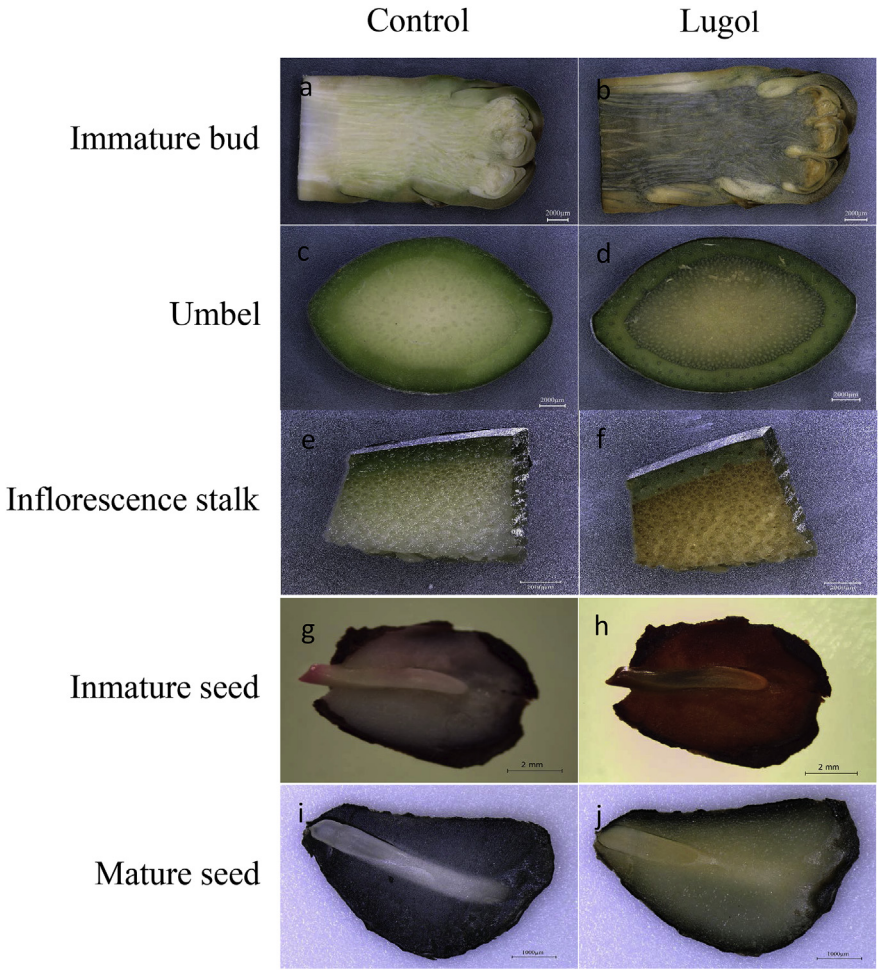

Fig. 4. Lugol staining of starch in floral tissues and seeds. a, c, e, g,i -unstained controls, b,d,f,g,j-lugol stained samples.

of the developing plantlet upon germination.

Levels of expression of several starch metabolism genes (both for synthesis and degradation of starch) are significantly lower in leaves than those observed for meristem tissue at both vegetative and reproductive stages with the exception of the SSS encoding genes which are expressed at similar levels in leaf and SAM tissue and show a significant drop in expression level in leaves of plants with a 10 cm inflorescence (IL). GBSS and AGPS also show lower expression in IL although this was not statistically significant, but could indicate that as the plant enters the reproductive stage less starch accumulates in leaf tissue and that carbohydrates produced by photosynthesis are channeled to the growing inflorescence.

A single gene AGPS shows a significant change in expression in meristem tissue at different stages of the vegetative to reproductive transition and interestingly this difference is noted between the vegetative stage (VM) and the initiation of the reproductive phase (SM). It

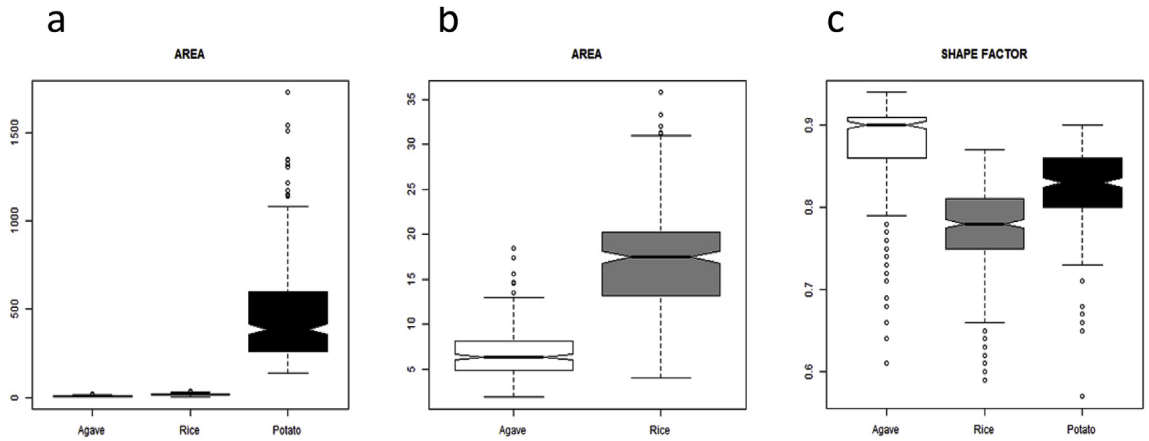

Fig. 5. Comparison of size and shape of starch grains between *A. tequilana*, rice and potato. a. Comparison of size (area um^2) of starch grains from *A. tequilana*, rice and potato. b. Data from a showing only rice and *A. tequilana* for comparison, c. Comparison of shapes of starch grains from *A. tequilana*, rice and potato. Value of 1 = perfect circle.

has been reported previously that at the SM stage, even though the inflorescence is not yet visible, umbel primordia are already visible around the SAM (Delgado Sandoval Sdel et al., 2012). AGPS is involved in the first step of starch synthesis and increased expression of this gene between VM and SM is consistent with the transient localization of starch in the PTM and umbel primordia as the inflorescence begins to develop.

The vegetative to reproductive transition is an important agronomic trait in *A. tequilana* since it signals the maturity of the plant and readiness for harvesting. However in the field this transition is difficult to predict and monitor and is currently identified by the "sinking" phenotype where the array of leaves changes from a domed to a sunken morphology. However, at this stage the SAM has already become an inflorescence meristem. A more precise method to identify the earliest stage of the transition would be of great benefit in commercial *Agave* production and expression levels of AGPS or levels of starch in the PTM surrounding the SAM could plausibly be developed as markers for this transition.

Expression levels of AGPS or levels of starch in the PTM surrounding the SAM could plausibly be developed as markers for this transition.

In mature leaves, starch is concentrated in the stomatal guard cells of both green and white (basal) leaf tissue and a few small starch grains are observed in the chloroplasts of cells closest to the photosynthetically active regions of *A. tequilana* leaves or associated with vascular tissue but not in inner leaf tissues or white (basal) leaf tissues. These results are consistent with the report of (Christopher and Holtum, 1996) that starch is not stored to a significant level in *A. guadalajarana* leaves.

Even in the PTM, *A. tequilana* starch grains are small in comparison to rice (*Oryza sativa*) a species reported to have some of the smallest starch grains of all plant species (Wani et al., 2012). This may reflect the transient accumulation of starch in *A. tequilana* where turnover of starch in actively growing tissues is relatively high as suggested by (Cabalkova et al., 2008) for Norway Spruce in comparison to other species where starch is used for long term carbohydrate storage such as potato. The spherical compact shape may also reflect a low amylose content in *A. tequilana* starch grains as suggested by Atkin et al. (1999).

PAS staining of stem tissue detects the presence of both starch and fructans and comparison with lugol stained samples suggests that in this organ the presence of each type of carbohydrate is mutually exclusive. This leads us to suggest that in *A. tequilana* and probably in most Agave species fructan accumulation accomplishes long term carbohydrate storage whereas starch is transiently stored and rapidly metabolized to provide energy for growth. Intriguingly both starch and fructans are detected in floral tissue of *A. tequilana* (present work and (Avila de Dios et al., 2015)). In Daylily, (*Hemerocallis hybrid*) (Bieleski, 1993) it has been reported that rather than an energy source, fructans in floral tissue function as osmotic regulators associated with flower opening. This would be consistent with the role of starch rather than fructans as the primary energy source for growth in floral tissue.

A general model for starch localization and function in relation to fructan metabolism is presented in Fig. 6. In summary we propose that, in photosynthetically active cells in leaves other than stomatal guard cells, starch transiently accumulates to low levels before being metabolized, leading to the synthesis of sucrose which can be transported to the PTM tissue of the stem where starch is again synthesized for short term storage. The sheath of starch which forms surrounding the expanded stem can be exploited for growth of leaves, developing roots, for stem expansion and for the development of asexual offsets from rhizomes and may also act as a reservoir to provide sucrose for fructan synthesis within the central stem tissue.

Starch also accumulates strongly in leaf primordia, providing carbohydrates for growth and both fructans and starch are present in floral tissue that is photosynthetically active in the immature, rapidly developing stages. Therefore precursors for starch synthesis may come directly from photosynthesis or from mobilization of sucrose or short fructan polymers from stem tissue. Lugol staining of embryo tissue specifically in tissue close to the SAM is consistent with the exploitation of starch as the primary carbohydrate source for growth in *A. tequilana*.

Strong expression of genes involved in fructan metabolism suggests that fructans are also synthesized *de novo* in floral organs however these polymers probably function as osmotic regulators rather than providers of carbohydrates for growth.

In conclusion, the results presented are consistent with differences in patterns of evolution of genes encoding enzymes involved in starch metabolism for non-gramineous monocotyledons in comparison to gramineous monocotyledons. The localization of starch in relation to stored fructans strongly suggests that starch is the primary carbohydrate exploited for growth throughout the life cycle of *A. tequilana*. More extensive analysis of the precise localization of fructans in different Agave organs and tissues is needed in order to confirm the putative functions of these molecules and it is essential to study the mobilization of sucrose and short fructan polymers between different plant organs and in different developmental stages in order to begin to understand more fully the interactions between starch and fructans at the molecular level.

Author contribution

Laura Zavala García carried out microscopy analysis of starch in different tissues, partially wrote and reviewed the manuscript.

Lino Sánchez Segura carried out and directed miscroscopy analysis and reviewed the manuscript.

Emmanuel Avila de Dios carried out all bioinformatic and expression analysis and reviewed the manuscript.

Arely Pérez López carried out analysis of PAS staining and starch localization in seeds and roots and reviewed the manuscript.

June Simpson directed the project, wrote and reviewed the manuscript.

Acknowledgements

Funding for this research was provided by the Consejo Nacional de Ciencia y Tecnología, (CONACYT) Mexico grant 132160. LZ received and undergraduate scholarship from the same project, EA and AP received postgraduate fellowships 367316 and 566173 respectively from CONACyT. We are indebted to Katia Gil Vega for technical and administrative support throughout the project and to Irapuato City Council for plant samples.

Appendix A. Supplementary data

a. Complete two year old plant showing the different tissues which were sampled. b. Dissected two year old plant showing internal tissues. c. Mature plant showing inflorescence and umbels. d. Close up image of flower buds and umbel tissue.

a. Rhodamine B staining and fluorescence emission spectra from potato starch. Circles represent the area where pixel intensities were measured. b. Average pixel intensities are presented for the emission wavelength in the graph.

a. AGPL- Adenosine Diphosphate Glucose Pyrophosphorylase large subunit, b. AGPS- Adenosine Diphosphate Glucose Pyrophosphorylase small subunit c. BAM-B amylase, d. A amylase, e.GBSS-Granule bound starch synthase, f. SSS-Soluble starch synthase, g. SBE-Starch branching enzyme, h. ISA-Isoamylase. The non-solid line indicates dicotyledons, the solid line indicates gramineous monocotyledons and the dashed line indicates non-gramineous monocotyledons. Species abreviations are as follows: Zm-*Zea mays*, Os-*Oryza sativa*, As-*Avena sativa*, Lp-*Lollium perenne*, At-*Arabidopsis thaliana*, Ma-*Musa acuminata*, St-*Solanum tuberosum*, Dc-*Daucus carota,* Bn-*Brassica napa*, Ca-*Capsicum annum*, Lj-*Lotus japonica*, Gm-*Glycine max*, Pv-*Phaseolus vulgaris*, Ac-*Allium cepa*, Eg-*Elaeis guianensis*, Ao-*Asparagus oficinalis*, Atq-*Agave tequilana* (boxed and

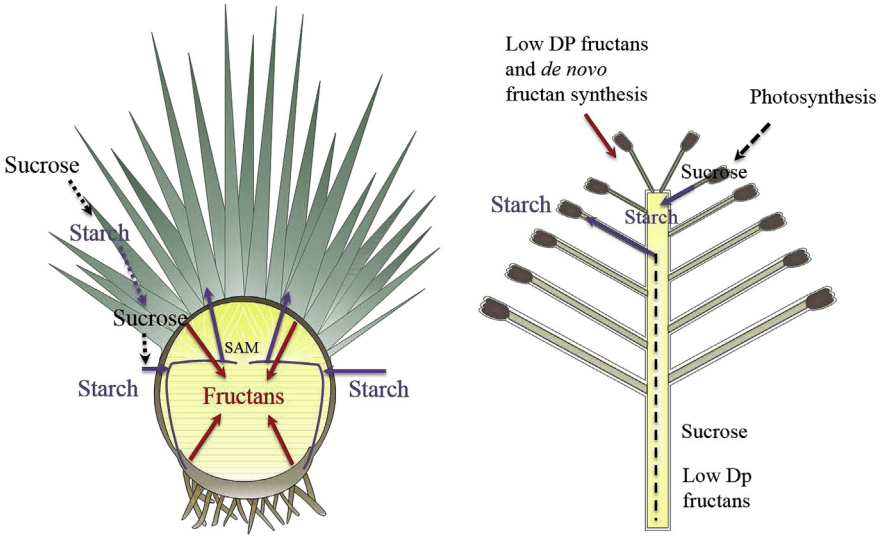

Fig. 6. Starch is the primary carbohydrate source for growth in *A. tequilana*. a. Localization of starch and fructans in vegetative tissue of *A. tequilana* plants, b. Localization of starch and fructans in reproductive structures of *A. tequilana.* Purple indicates sites of starch synthesis, dotted black lines indicate putative mobility of sucrose and or short fructan polymers. Solid purple arrows indicate consumption of starch for growth of leaves, stem and rhizomes. Red arrows indicate putative consumption of starch for synthesis of fructans. The purple lines around the stem indicate starch accumulation at the PTM. (For interpretation of the references to color in this figure legend, the reader is referred to the Web version of this article.)

shown in blue), Nt-*Nicotiana tabacum*, Atrich-*Amborella trichopoda*, Cs-*Camellia sinensis*, Gh-*Gossypium hirsutum*, Ta-*Triticum aestivum*, Hv-*Hordeum vulgare*, Md-*Malus domesticus*, Cc-*Cafe canephora*, Gs-*Glycine soya*, Sb-*Sorghum bicolor*, Cp-*Carica papaya*, Ps-*Pisum sativum*, Mt-*Medicago truncatula*,

The number of transcripts are presented as mean transcripts pero million based on three indpendant replicas. AGPL- Adenosine Diphosphate Glucose Pyrophosphorylase large subunit, AGPS-Adenosine Diphosphate Glucose Pyrophosphorylase small subunit BAM B-amylase, GBSS-Granule bound starch synthase, SSS-Soluble starch synthase, ISA-Isoamylase. VL-vegetative leaf, SL-leaf in 1st stage of bolting, IL-Leaf from plant with 1m inflorescence, VM-vegetative SAM, SM-SAM in 1st stage of bolting, IM-SAM from plant with 1m inflorescence. * indicates significant difference in expression levels in comparison to other samples.

a, c and e Transverse sections of *A. tequilana* stem tissue, a-unstained control, c, stained with lugol. e-stained with PAS. b, d and f Transverse sections of *A. tequilana* rhizome tissue. b-unstained control, d-stained with lugol, f-stained with PAS.

a-d leaf primordia, e-h Vascular bundles, i-l Mid-section green leaf, m-p Mid-section white leaf, q-t Mid-section of root and d control and background images for Fig. 3 e and f respectively. TMPT-Transmision PhotoMultiplier Tube. Circles indicate chloroplasts showing rhodamine fluoescence, arrows indicate stomata.

Left hand panel-dissected unstained mature seed, right hand panel-diseected PAS stained mature seed. E indicates the embryo.

Supplementary data related to this article can be found at https://doi.org/10.1016/j.plaphy.2018.08.011.

References

Atkin, N.J., Cheng, S.L., Abeysekera, R.M., Robards, A.W., 1999. Localisation of amylose and amylopectin in starch granules using enzyme-gold labelling. Starch 51, 163–172.

Avila de Dios, E., Gomez Vargas, A.D., Damian Santos, M.L., Simpson, J., 2015. New insights into plant glycoside hydrolase family 32 in Agave species. Front. Plant Sci. 6, 594.

Bieleski, R.L., 1993. Fructan hydrolysis drives petal expansion in the ephemeral daylily flower. Plant Physiol. 103, 213–219.

Brocklebank, K.J., Hendry, G.A.F., 1989. Characteristics of plant-species which store different types of reserve carbohydrates. New Phytol. 112, 255–260.

Cabalkova, J., Pribyl, J., Skladal, P., Kulich, P., Chmelik, J., 2008. Size, shape and surface morphology of starch granules from Norway spruce needles revealed by transmission electron microscopy and atomic force microscopy: effects of elevated CO(2) concentration. Tree Physiol. 28, 1593–1599.

Cattai, M.B., Menezes, N.L., 2010. Primary and secondary thickening in the stem of Cordyline fruticosa. An. Acad. Bras. Cienc. 82, 653–662.

Christopher, J.T., Holtum, J., 1996. Patterns of carbon partitioning in leaves of crassulacean acid metabolism species during deacidification. Plant Physiol. 112, 393–399.

Comparot-Moss, S., Denyer, K., 2009. The evolution of the starch biosynthetic pathway in cereals and other grasses. J. Exp. Bot. 60, 2481–2492.

Cushman, J.C., Davis, S.C., Yang, X., Borland, A.M., 2015. Development and use of bioenergy feedstocks for semi-arid and arid lands. J. Exp. Bot. 66, 4177–4193.

Davis, S.C., Dohleman, F.G., Long, S.P., 2011. The global potential for Agave as a biofuel feedstock. Gcb Bioenergy 3, 68–78.

Delgado Sandoval Sdel, C., Abraham Juarez, M.J., Simpson, J., 2012. Agave tequilana MADS genes show novel expression patterns in meristems, developing bulbils and floral organs. Sex. Plant Reprod. 25, 11–26.

Van den Ende, W., 2013. Multifunctional fructans and raffinose family oligosaccharides. Front. Plant Sci. 4, 247.

Van den Ende, W., 2014. Sugars take a central position in plant growth, development and, stress responses. A focus on apical dominance. Front. Plant Sci. 5, 313.

Van den Ende, W., Valluru, R., 2009. Sucrose, sucrosyl oligosaccharides, and oxidative stress: scavenging and salvaging? J. Exp. Bot. 60, 9–18.

Van den Ende, W., De Coninck, B., Van Laere, A., 2004. Plant fructan exohydrolases: a role in signaling and defense? Trends Plant Sci. 9, 523–528.

Ernst, M., Krug, H., 1998. Seasonal growth and development of asparagus (Asparagus officinalis L.). III. The effect of temperature and water stress on carbohydrate content in storage roots and rhizome buds. Gartenbauwissenschaft 63, 202–208.

Ernst, M.K., Chatterton, N.J., Harrison, P.A., Matitschka, G., 1998. Characterization of fructan oligomers from species of the genus Allium L. J. Plant Physiol. 153, 53–60.

Ernst, M.K., Praeger, U., Weichmann, J., 2003. Effect of low oxygen storage on carbohydrate changes in onion (Allium cepa var. cepa) bulbs. Eur. J. Hortic. Sci. 68, 59–62.

Escobar-Guzmán, R., Zamudio-hernández, F., Gil-Vega, K., Simpson, J., 2008. Seed production and gametophyte formation in *Agave tequilana* and *Agave americana*. Botany 86, 1343–1353.

García, A., 2011. Flora del Valle de Tehuacán. Universidad Nacional Autónoma de México, Mexico City.

García-Mendoza, A., 1992. Con Sabor a Maguey, 1 ed. Universidad Nacional Autónoma de México, Mexico City.

García-Mendoza, A., 2000. Distribution of *Agave* (agavaceae) in Mexico. Cactus Succulent J. 74, 177–188.

Gentry, H.S., 1982. Agaves of continental North America. University of Arizona Press, Tucson.

Hendry, G., 1987. The ecological significance of fructan in a contemporary flora. New Phytol. 106, 201–216.

Hendry, G.A.F., 1993. Evolutionary origins and natural functions of fructans - a climatological, biogeographic and mechanistic appraisal. New Phytol. 123, 3–14.

James, M.G., Denyer, K., Myers, A.M., 2003. Starch synthesis in the cereal endosperm. Curr. Opin. Plant Biol. 6, 215–222.

Kearse, M., Moir, R., Wilson, A., Stones-Havas, S., Cheung, M., Sturrock, S., Buxton, S., Cooper, A., Markowitz, S., Duran, C., Thierer, T., Ashton, B., Meintjes, P., Drummond, A., 2012. Geneious Basic: an integrated and extendable desktop software platform for the organization and analysis of sequence data. Bioinformatics 28, 1647–1649.

Li, Z., Sun, F., Xu, S., Chu, X., Mukai, Y., Yamamoto, M., Ali, S., Rampling, L., Kosar-Hashemi, B., Rahman, S., Morell, M.K., 2003. The structural organisation of the gene encoding class II starch synthase of wheat and barley and the evolution of the genes encoding starch synthases in plants. Funct. Integr. Genom. 3, 76–85.

Li, C., Li, Q.G., Dunwell, J.M., Zhang, Y.M., 2012. Divergent evolutionary pattern of starch biosynthetic pathway genes in grasses and dicots. Mol. Biol. Evol. 29, 3227–3236.

Liu, L., Ramsay, T., Zinkgraf, M., Sundell, D., Street, N.R., Filkov, V., Groover, A., 2015. A resource for characterizing genome-wide binding and putative target genes of transcription factors expressed during secondary growth and wood formation in Populus. Plant J. 82, 887–898.

Mancilla-Margalli, N.A., Lopez, M.G., 2006. Water-soluble carbohydrates and fructan structure patterns from Agave and Dasylirion species. J. Agric. Food Chem. 54, 7832–7839.

Mancilla-Margalli, N.A., López, M.G., 2006. Water-soluble carbohydrates and fructan structure patterns from Agave and Dasylirion species. J. Agric. Food Chem. 54, 7832–7839.

de Menezes, N.L., Silva, D.C., Arruda, R.C., Melo-de-Pinna, G.F., Cardoso, V.A., Castro, N.M., Scatena, V.L., Scremin-Dias, E., 2005. Meristematic activity of the Endodermis and the Pericycle in the primary thickening in monocotyledons: considerations on the "PTM". An. Acad. Bras. Cienc. 77, 259–274.

Sánchez-Segura, L., Tellez-Medina, D.I., Evangelista-Lozano, G.-A.S., Hernandez-Sanchez, A.-B.E.,L.H., Jiménez Aparicio, A.R., Gutierrez-Lopez, G.F., 2015. Morpho-structural description of epidermal tissues related to pungency of Capsicum species. J. Food Eng. 152, 95–104.

Schnabl, H., 1980. CO2 and malate metabolism in starch-containing and starch-lacking guard-cell protoplasts. Planta 149, 52–58.

Schnabl, H., Ziegler, H., 1977. The mechanism of stomatal movement in Allium cepa L. Planta 136, 37–43.

Schnabl, H., Bornman, C.H., Ziegler, H., 1978. Studies on isolated starch-containing (Vicia faba) and starch-deficient (Allium cepa) guard cell protoplasts. Planta 143, 33–39.

Scofield, G.N., Ruuska, S.A., Aoki, N., Lewis, D.C., Tabe, L.M., Jenkins, C.L., 2009. Starch storage in the stems of wheat plants: localization and temporal changes. Ann. Bot. 103, 859–868.

Wang, N., Nobel, P.S., 1998. Phloem transport of fructans in the crassulacean acid metabolism species Agave deserti. Plant Physiol. 116, 709–714.

Wani, A.A., Singh, P., Shah, M.A., Schweiggert-Weisz, U., Gul, K., Wani, I.A., 2012. Rice starch diversity: effects on structural, morphological, thermal, and physicochemical properties—a review. Compr. Rev. Food Sci. Food Saf. 11, 417–436.

Yang, X., Cushman, J.C., Borland, A.M., Edwards, E.J., Wullschleger, S.D., Tuskan, G.A., Owen, N.A., Griffiths, H., Smith, J.A., De Paoli, H.C., Weston, D.J., Cottingham, R., Hartwell, J., Davis, S.C., Silvera, K., Ming, R., Schlauch, K., Abraham, P., Stewart, J.R., Guo, H.B., Albion, R., Ha, J., Lim, S.D., Wone, B.W., Yim, W.C., Garcia, T., Mayer, J.A., Petereit, J., Nair, S.S., Casey, E., Hettich, R.L., Ceusters, J., Ranjan, P., Palla, K.J., Yin, H., Reyes-Garcia, C., Andrade, J.L., Freschi, L., Beltran, J.D., Dever, L.V., Boxall, S.F., Waller, J., Davies, J., Bupphada, P., Kadu, N., Winter, K., Sage, R.F., Aguilar, C.N., Schmutz, J., Jenkins, J., Holtum, J.A., 2015. A roadmap for research on crassulacean acid metabolism (CAM) to enhance sustainable food and bioenergy production in a hotter, drier world. New Phytol. 207, 491–504.

Zeeman, S.C., Kossmann, J., Smith, A.M., 2010. Starch: its metabolism, evolution, and biotechnological modification in plants. Annu. Rev. Plant Biol. 61, 209–234.

Zhang, C., Zhang, H., Zhan, Z., Liu, B., Chen, Z., Liang, Y., 2016. Transcriptome analysis of sucrose metabolism during bulb swelling and development in onion (Allium cepa l.). Front. Plant Sci. 7, 1425.